Progressive Collapse Assessment of Steel Moment Frames with the RBS Connections by Considering Different Seismicity and Ductility Levels

Behzad Rezaee, Payam Tehrani*, Behrouz Behnam

Department of Civil Engineering, Amirkabir university of technology, Tehran, Iran

Abstract:

Extreme events such as earthquakes can damage vertical load-bearing elements, particularly columns, potentially triggering progressive collapse in building systems. This vulnerability is more pronounced in steel moment-resisting frames due to their relatively limited redundancy. Although previous studies have investigated the progressive collapse behavior of moment frames under different seismicity and ductility levels, the influence of key seismic design parameters—such as reduced beam section (RBS) connections, ductility level, and the strong column–weak beam (SC–WB) principle—remains insufficiently understood, with conflicting findings reported in the literature. This study aims to systematically evaluate the role of these seismic design parameters in the progressive collapse response of steel moment frames. To this end, 5-, 10-, and 15-story buildings were designed for low, medium, and high seismicity levels, considering both intermediate and special moment frames with RBS connections. A total of 340 column removal scenarios were analyzed using nonlinear dynamic analysis in OpenSees, employing a lumped plasticity modeling approach. Structural performance was assessed in terms of damage percentage index (DPI), ductility demand, and vertical nodal displacement. The results indicate that ductility demands in all cases remained within code-prescribed performance limits, suggesting that RBS connections provide adequate robustness against progressive collapse under column removal scenarios. However, neglecting the SC–WB principle significantly increases ductility demand and vertical displacement, by up to 1.83 and 1.56 times, respectively, in critical cases. Furthermore, the ductility level of the lateral-resisting system strongly influences structural response, particularly in medium seismicity conditions, where weaker member sizes lead to reduced robustness and amplified deformation demands.

Keywords:

Progressive collapse, the RBS connection, nonlinear dynamic analysis, special moment frames, strong column-weak beam.

*Corresponding Author, Email address: payam.tehrani@aut.ac.ir

1. Introduction

The structural damage observed during the 1994 Northridge and 1995 Kobe earthquakes prompted significant changes in seismic design for lateral-resisting systems, particularly steel moment frames[1]. Notable failures occurred in beam-to-column moment connections, including fractures in bottom flange welds and cracking in column flanges [2-4]. To address these issues, various strategies were proposed, such as relocating plastic hinge positions, following the "strong column-weak beam" philosophy outlined in regulations. The plastic hinge relocation can involve either strengthening connections or implementing weaking techniques such as the reduced beam section (RBS) connections [5, 6]. Moreover, beam-to-column connections are crucial components for ensuring structural stability against various severe loadings, including local explosions, impact loadings, terrorist attacks, and fires. These loading patterns cause localized damage, potentially leading to beam or column removal, which propagates throughout the structure and results in global collapse [7-9]. Following the World Trade Center collapse[4], designing buildings to resist progressive collapse gained significant attention, leading to modern regulations such as GSA and UFC aimed for enhancing structural resilience. These regulations provide different static and dynamic procedures to simulate the dynamic behavior of progressive collapse [10, 11].

Numerous studies have investigated how connection type affects the progressive collapse resistance of structures. For instance, Kim et al. [4] assessed RBS, Welded Unreinforced Flange-Welded Web (WUF-W), and Welded Cover Plated Flanges (WCPF) connections under various column removal scenarios, finding that structures with RBS connections were generally less resist than those with WUF-W and WCPF connections. Similarly, Park et al. [12] analyzed RBS, Welded Unreinforced Flange-Bolted Web (WUF-B), and WCPF connections through pushdown and fragility analyses. Their findings indicated that RBS connections were robust enough to resist column removal. Although both Park et al. and Kim et al. used distributed plasticity in the OpenSees software [13], their results appear contradictory.

Khandelwal and El-Tawil [14] studied a special moment frame with an RBS connection designed for high seismicity alongside an intermediate frame with a WUF-W connection for moderate seismicity. They concluded that the special frame structure exhibited greater strength against progressive collapse. Hadidi et al. [15] utilized optimization techniques to explore the design parameters of steel moment frames. They demonstrated that SidePlate moment connections result in structures that are resistant to progressive collapse while using lighter elements. Faridmehr et al. [16] examined the seismic and collapse behavior of SidePlate moment connections, revealing that these connections have sufficient rotational capacity to withstand progressive failure. Lee et al. [17, 18] evaluated the performance of moment steel frames with two different connection types of RBS and WUF-B under column removal scenarios. They showed that the RBS connections had better progressive collapse resistance compared to the WUF-B connections. Also, they showed that moment frames with higher ductility levels are more vulnerable to progressive collapse.

In a numerical-experimental study, Chen et al. [19] investigated the progressive collapse in moment frames with RBS connections, demonstrating that these connections effectively prevent the rapid failure of the beam-to-column connection. Additional studies [12, 14, 17, 18, 20, 21] have shown that, overall, RBS connections had greater rotational capacity and ductility compared to other conventional connection types. Meng et al. [22] added V-shaped plates at the reduced part of the RBS connection and proposed a novel configuration that can improve the bearing capacity while the catenary action is fully developed. Semsarha et al. [23, 24] showed that the structures with the higher ductility level, are weaker during the column removal scenarios following an earthquake. Zhang et al. [25] investigated the post-fire progressive collapse of substructures with the RBS connection. They showed that under the fire loading condition the RBS connection don't have enough capability and robustness to relocate the plastic hinges. Rezaee et al. [26] demonstrated that special moment frames equipped with RBS connections exhibit sufficient robustness and superior performance under post-earthquake progressive collapse scenarios involving column removal. A summary of the key findings from previous studies on progressive collapse is presented in Table 1.

Table 1: Summery of previous studies

No	Researchers	Type of evaluation	General subject	Controlling parameters
1	Kim et al (2009) [4]	Numerical	Evaluation the progressive collapse behavior of RBS, WCFP, WUF-W connections	Vertical displacement, ductility demand
2	Park & Kim (2010)[12]	Numerical	Fragility analysis of moment frames considering RBS ،WUF-B ،WCFP connections	Load factor, plastic rotation, vertical displacement
3	Khandelwal & El-Tawil(2011) [14]	Numerical	Comparison the effect of type and connections in the collapse response of moment frames	Load factor, collapse mode
4	Faridmehr et al (2015) [26]	Experimental-numerical	Seismic and progressive collapse behavior of the side plate connections	Plastic rotation, bending strength, rotation capacity
5	Dinu et al (2017) [20]	Experimental-numerical	Progressive collapse resistance of different moment connections	Bending capacity, axial resistance, vertical displacement
6	Behnam et al (2019) [27]	Numerical	Seismic progressive collapse assessment of moment frames using beam removal scenarios	Rotation of beam, DCR, axial and moment responses of columns
7	Chen et al (2020) [19]	Experimental-numerical	Evaluation the behavior of RBS connections under column removal scenario	Design parameters, axial resistance, vertical displacement
8	Qian et al (2020) [21]	Experimental-numerical	Comparison progressive collapse behavior of RBS and GBS connections	Axial resistance, rotation, vertical displacement, design configurations
9	Wang et al (2020) [28]	Experimental-numerical	Parametric assessment of various moment connections under middle column removal case	Rotation capacity, axial resistance

10	Lee et al (2018, 2021) [17, 18]	Numerical	Comparison the collapse behavior of RBS and WUF-B connections considering various response factors	Load factor, rotation, vertical displacements
12	Semsarha et al (2021,2023) [23, 24]	Numerical	Post-earthquake progressive collapse assessment of moment frames using 2D and 3D models	Vertical displacements, ductility demands, D/C ratio, Failure percentage
13	Rezaee et al [29]	Numerical	Post-earthquake progressive collapse assessment of moment frames using rigid and RBS connections	Vertical displacements, ductility demands, Failure percentage
14	Current study	Numerical	Progressive collapse behavior of RBS connection of low-, mid-, and high-rise buildings under various seismic design parameters	Vertical displacements, ductility demand, DPI

While extensive studies have assessed the progressive collapse response of moment frames with various connections, including the RBS connection, there is limited research on structural behavior under differing seismicity and ductility levels. For instance, Park and Kim [12] and Rezaee et al. [26] reported that RBS connections provide adequate robustness under both pre- and post-earthquake progressive collapse scenarios. In contrast, Kim et al. [4] indicated that such connections may exhibit insufficient resistance under column removal conditions. Furthermore, Semsarha et al. [24] and Lee et al. [18] observed that moment frames designed with higher response modification factors (R factors) may perform less favorably under progressive collapse due to the reduced size and strength of structural members. Conversely, Rezaee et al. [26] and Khandelwal et al. [14] demonstrated that incorporating RBS connections within special moment frames can result in acceptable performance under both progressive collapse and post-earthquake scenarios.

In addition, most existing studies have primarily focused on low- and mid-rise structures, whereas the behavior of taller buildings—where load redistribution mechanisms can differ significantly—has received comparatively limited attention. Although seismic design principles such as the strong column–weak beam (SC–WB) criterion are well established for improving seismic performance, their specific influence on progressive collapse behavior across different seismicity levels remains insufficiently understood. Moreover, previous studies have generally examined the effects of individual parameters, such as R factor, seismicity level, or connection type, without considering their combined influence. Therefore, a comprehensive parametric investigation that simultaneously accounts for seismicity level, ductility level (R factor), RBS connections, building height, and the SC–WB principle is still lacking in the literature.

In this study, a lumped plasticity modeling approach is adopted for the progressive collapse assessment of steel moment frames with RBS connections under gravity-driven column removal scenarios. While distributed plasticity models are commonly employed to capture catenary action, lumped plasticity models provide an efficient and practical framework for evaluating hinge performance, identifying critical deformation demands, and supporting pre- and post-earthquake progressive collapse assessments [23, 24, 26]. Furthermore, the performance levels of plastic hinges in such models offer valuable insight into the global structural response, enabling meaningful comparison with results obtained from more detailed modeling approaches.

Accordingly, this study aims to investigate the impact of RBS connections on the progressive collapse potential of steel moment-resisting frames across different seismicity levels and ductility demands, considering low-, mid-, and high-rise buildings within a unified analytical framework. While progressive collapse can result from various causes, this research focuses solely on column removal, disregarding its underlying reasons. 19 structures, comprising 5, 10 and 15 stories were evaluated under corner and middle column removal scenarios (340 cases). The structures are designed according to ASCE7-16 standard [30] for gravity and seismic loads. Structural components are designed per AISC360-16 and AISC341-16 [31, 32] , with RBS connections based on AISC358-16 [33]. The structural system includes special moment

frames (SMF) and intermediate moment frames (IMF) under low, medium, and high seismicity levels. Additionally, four frames are designed without the "strong column-weak beam" principle to evaluate the role of seismic considerations in collapse response. Nonlinear dynamic procedures per UFC guidelines are used to simulate progressive collapse scenarios with a focus on ductility demands, vertical nodal displacements of the removed column, and damage percentage index (DPI) as controlling parameters for assessing collapse behavior.

2- Materials and methods

2-1-Methodology

The overall procedure adopted in this study is illustrated in Fig. 1. Initially, the structures were designed to resist both gravity and seismic loads. Progressive collapse assessment was then performed using the Alternate Path Method (APM) in accordance with the UFC guidelines [11], in which column removal scenarios are simulated through nonlinear dynamic analysis.

As shown in Fig. 2, the analysis procedure consists of several steps. First, the nonlinear model was developed and subjected to gravity loading. The axial (P), shear (V), and moment (M) reactions of the target column were then recorded. Subsequently, the selected column was removed from the model to initiate the progressive collapse scenario. Following column removal, two simultaneous loading processes were applied. On the one hand, gravity loads were increased linearly over a duration of 5 seconds and then maintained constant in accordance with the UFC load combination. On the other hand, the previously recorded column reactions (P, V, M) were applied at the node above the removed column and increased linearly over the same 5-second period until reaching their maximum values. These reactions were then held constant for an additional 2 seconds to ensure numerical stability. Finally, the applied reactions were suddenly released to simulate the instantaneous loss of the column.

Afterward, key response parameters—including the damage percentage index (DPI), ductility demand, and vertical nodal displacement—were monitored to evaluate the structural robustness. Figures 3(a)–3(d)

present the primary structural model and representative column removal scenarios for a 5-story building modeled in OpenSees.

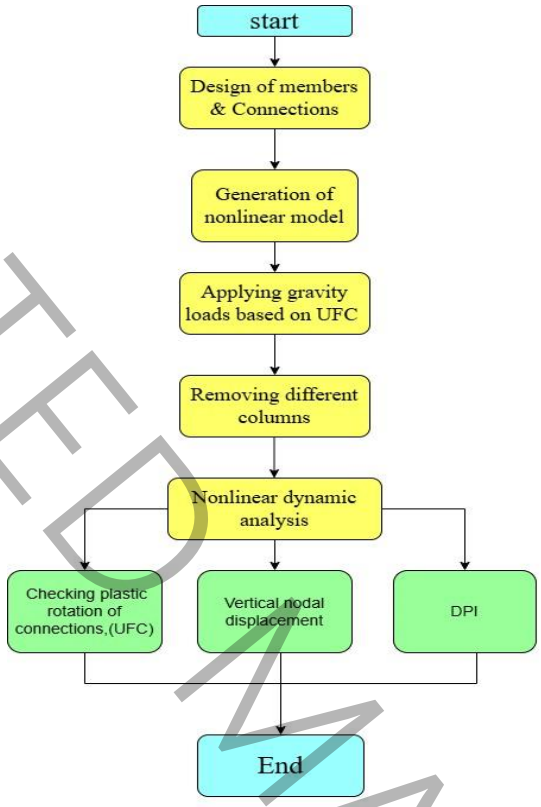

Fig. 1. Steps of progressive collapse assessment of structures under column removal scenarios

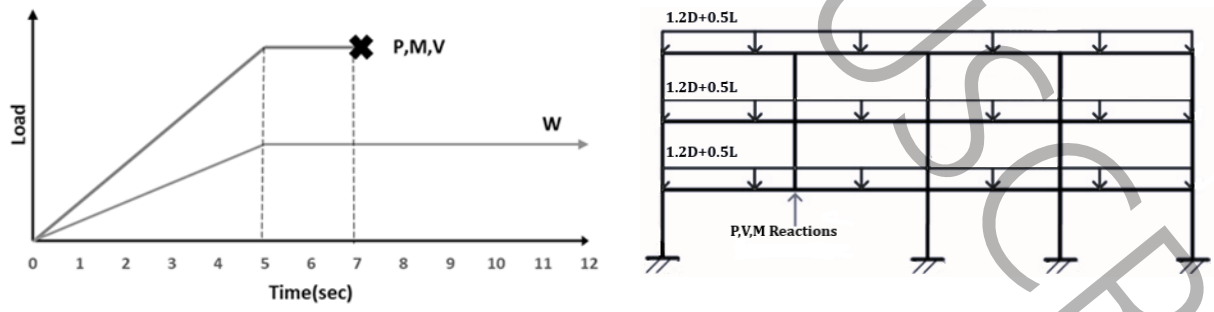

(a) **(b)**

Fig. 2. Concept of progressive collapse loading and column removal [34]

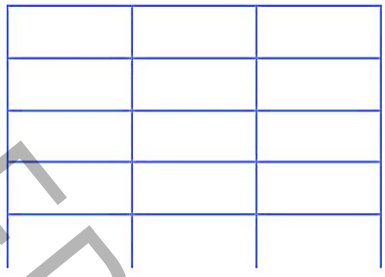

(a) Primary structure

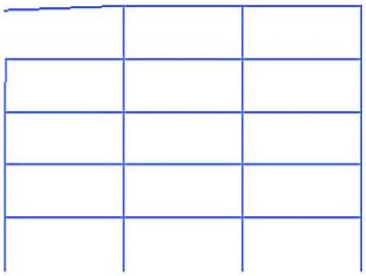

(b) Corner column removal in the last story

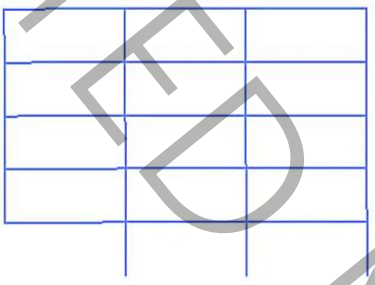

(c) Corner column removal in the first story

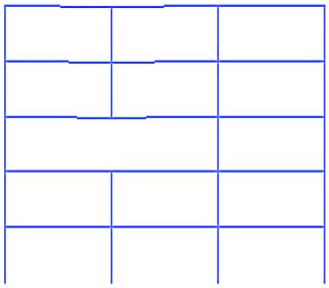

(d) Middle column removal in the third story

Fig. 3. Column removal scenarios in OpenSees

The UFC recommends that plastic rotations adhere to the guidelines from the previous edition of ASCE41, which lacks a performance-level category. Therefore, this study evaluates ductility demands according to both UFC and ASCE41-23 [35]. Nonlinear modeling parameters and acceptance criteria are detailed in Table A1 (Appendix A). The acceptance criterion for the Life Safety (LS) level in ASCE41-23 is similar to that in the UFC, though the UFC criterion is slightly more conservative.

2-2-Selecting the prototype building

In this study, in the tables and figures, 'S' represents the number of floors, while 'B' and 'BL' denote the number and length of the bays, respectively. The behavior factor 'R' is established at 8 for special moment frames and 4.5 for intermediate moment frames. The designs account for three levels of seismicity: low seismicity in Las Vegas (S1=0.193 and Ss=0.59), medium seismicity in Portland (S1=0.396 and Ss=0.887), and high seismicity in San Francisco (S1=0.6 and Ss=1.5). Four special moment frame buildings were

designed without following the strong column-weak beam (WSC-WB) principle. Each structure consists of 3 bays, each measuring 6 meters in length, with a floor height of 3.2 meters. All designs assume soil type C, as specified by the ASCE7-16 regulations. The flooring system uses a one-way slab with a thickness of 10 cm. Fig. 4 illustrates a sample structure in both horizontal and vertical planes for a 5-story building. Further details on the beam and column sections can be found in Appendix B.

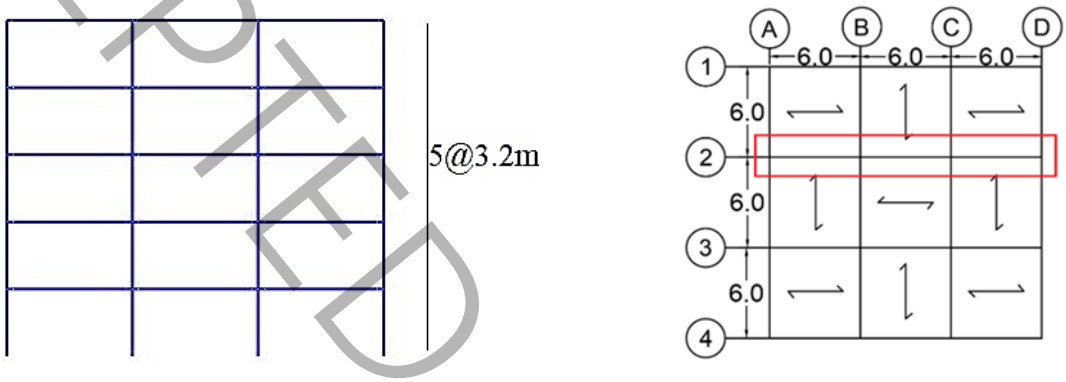

a) Side view b) Plan view

Fig. 4: Plan and side views of the 5-story building

The dead and live loads for all floors, excluding the roof, are 5.9 kN/m² and 2.5 kN/m², respectively. For the roof, the dead load is 4.9 kN/m², while the live load is 1.5 kN/m². Additionally, the load from the surrounding walls is set at 7.36 kN/m. The seismic weight considers 100% of the dead load and 20% of the live load. The yield and ultimate stress of the steel sections are 240 MPa and 370 MPa, respectively, with a Poisson's ratio of 0.3 for steel. The compressive strength of the concrete slab is assumed to be 25 MPa, and the Poisson's ratio for concrete is 0.2.

The geometry configuration of the RBS connection is shown in Fig. 5. The design procedure is based on a trial-and-error approach. Three design parameters of a, b, and c are considered, where $a=0.6b_{bf}$, $b=0.7d_b$, and $c=0.25b_{bf}$; and considering that b_{bf} is the beam width and d_b is the beam depth. These are considered to

satisfy the demand ratio to the beam's capacity [33]. The geometric parameters of the RBS connections for the various beams are summarized in Table C1 (Appendix C).

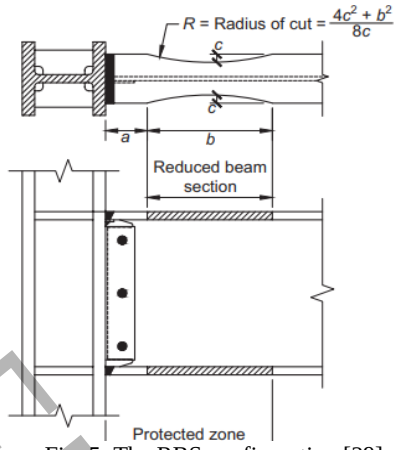

Fig. 5: The RBS configuration [29]

2-3- Nonlinear modeling

The nonlinear modeling and analysis were conducted in the OpenSees software [13] and the lumped plasticity model was selected for the assessment. To capture the inelastic behavior of the structure, the concentrated plastic hinges are considered as the zero length rotational springs in the model. The Bilinear material is used to consider the modified Ibarra-Medina-Krawinkler (IK) deterioration model [36, 37].The details of the nonlinear model are shown in Fig. 6(a). In this figure, θ_y, θ_c,θ_r, θ_u, M_c, M_y are effective yield rotation, capping rotation, rotation of residual strength, ultimate rotation, capping strength and effective yield strength, respectively, and K_e is elastic stiffness. To define the nonlinear parameters of hinges, the equations from Lignos et al studies and NIST recommendations were used. For the beams and columns, the equations of wide flange and HSS sections were used. The M_c/M_y ratio was assumed 1.1. For the M_y, the expected plastic moment $M_{p,exp}$ was multiplied by β, which is 1.2 for the beams with the RBS connections. Also, the residual strength was assumed to be 0.4 My. Additionally, it was assumed that plastic hinges, modeled as zero-length rotational springs, are placed at the ends of the columns. For the beams, however, the hinge location is defined as Sh = a + b/2. This configuration is depicted in Fig. 6(b). The middle element is considered elastic with the elasticBeamColumn command. were applied in accordance with the recommendations of Zareian & Medina for steel moment frames [38], utilizing a factor of n=10. In this

procedure, the rotational stiffness at the beam end and the moment of inertia of the elasticBeamColumn element are scaled by factors of n and ((n+1)/n), respectively. Here, n represents the ratio of the rotational spring stiffness of the beam to its elastic stiffness.

Also, the geometric transfer of beams is considered with Linear command and columns with P-Delta command. In this model, a Rayleigh damping ratio of 5% is adopted. Within this framework, the damping matrix, C, is formulated as a combination of mass-proportional and stiffness-proportional terms [39], as presented in Eq. (1),

$$C = \alpha M + \beta K \tag{1}$$

The α and β also are defined in Eq. (2) and Eq. (3) respectively. where the ω_1 and ω_2 are first and second mode frequences.

$$\alpha = \frac{2 \times 0.05 \times \omega 1 \times \omega 2}{\omega 1 + \omega 2} \tag{2}$$

$$\beta = \frac{2 \times 0.05}{\omega 1 + \omega 2} \tag{3}$$

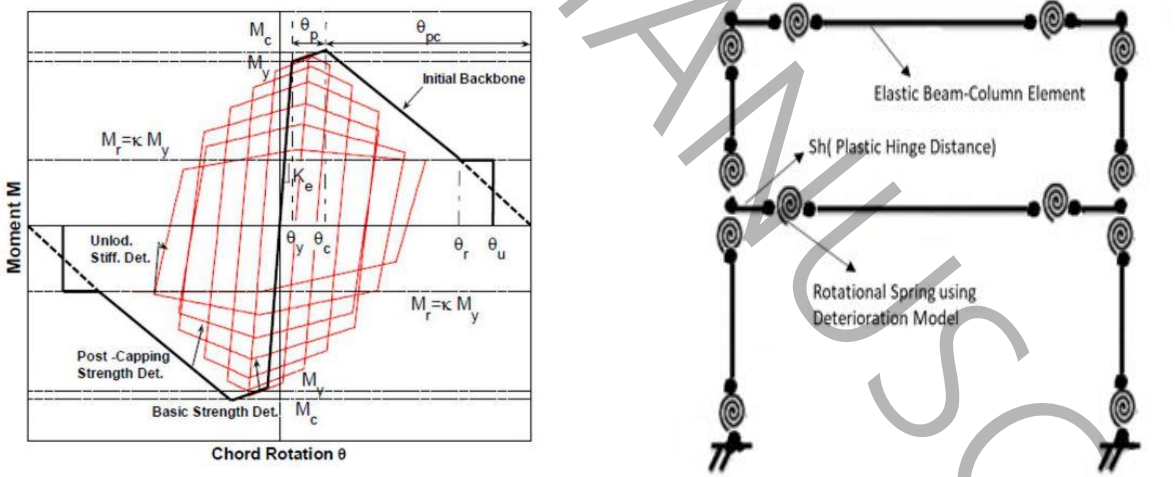

(a) IK deterioration model (b) Nonlinear concentrated hinge model

Fig. 6: Nonlinear modeling parameters

2-3-1-Model verification

To verify the nonlinear model, a spring column was selected based on the experimental results examined by Lignos et al [40, 41]. The study involved a large-scale experiment to evaluate the behavior of steel wide-flange columns under monotonic and cyclic loading protocols. Different prototypes and axial ratios were considered. Based on the experimental results, Lignos et al. modified and recommended some relationships for defining nonlinear parameters in the lumped plasticity models. To ensure about the validation of numerical models, a W14x82 column specimen with Pg/Pye ratios of 0.3 and 0.5 were selected for the assessment. The numerical model incorporated a rotational spring and an elastic beam-column element to capture the lumped plasticity behavior of the column. For monotonic loading, a target displacement was established based on experimental data. Based on the results in Fig. 7, for Pg/Pye = 0.3, the peak moment of the numerical model was 8,800 kips.in, compared to 9,000 kips.in for the experimental results, indicating an error of 2.22%. Furthermore, the ultimate rotations for the numerical and experimental results were 0.15 and 0.16 rad, respectively (error = 6.25%). For Pg/Pye = 0.5, the peak moments of the experimental and numerical models were 6,300 and 6,211 kips-in, respectively, corresponding to an error of 1.41%. Additionally, the ultimate rotations were 0.15 and 0.145 rad, showing an error of less than 1%. Consequently, the numerical and experimental results demonstrate strong agreement

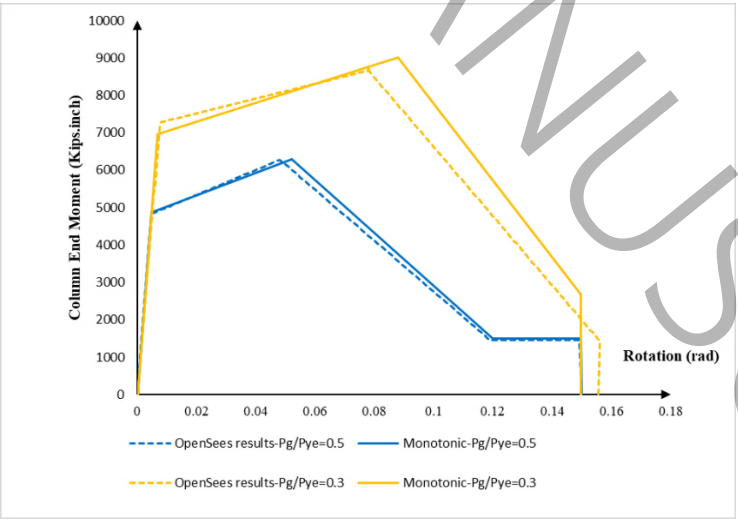

Fig. 7: Verification of the experimental results and numerical model [40, 41]

2-3-2-Result validation and model sensitivity

To assess the potential sensitivity of the results and verify the model's behavior under progressive collapse loading, a sensitivity analysis was conducted. For this purpose, the case designated as 5S.3B.6BL.8R.HER under the 5th column removal scenario was selected. Subsequently, the effects of various modifications were investigated, including the removal of lateral bracing from the beams on the last (5^{th}) floor, changing the nfactor from 10 to 5 [38], altering the geometric transformation from linear (beams) and P-Delta (columns) to Corotational, amplifying the axial load of the top-floor columns (two times larger), and reducing the beam length by 1 meter. The resulting changes in ductility demand and vertical nodal displacement were monitored. The values of ductility demands and vertical displacements for the modified models, along with their respective differences, are presented in Table 2. The results indicate that alterations in all parameters resulted in a difference of less than 8% in the worst-case scenario. This evaluation demonstrates that variations in beam length and the nfactor have a more pronounced effect on the results compared to other parameters. Furthermore, given the absence of significant changes in the new values, it can be concluded that the model effectively captures these variations and performs as intended. It is worth mentioning that the alterations didn't change the damage percentage in none of cases.

Table. 2: Sensitivity assessment

Ductility demand		
Params	Modified value	Difference %
Length	0.082	6.10
Lateral brace	0.088	1.14
Axial ratio	0.087	0.34
Geo Trans	0.087	0.46
nfac	0.090	3.33
Vertical displacement		
Params	Modified value	Difference %
Length	6.00	7.38
Lateral brace	6.28	4.30
Axial ratio	6.60	0.76
Geo Trans	6.56	0.15
nfact	6.18	5.99

In addition to the damage percentage, the overall response trends—including vertical displacement and ductility demand—were found to be consistent with the reference study, further supporting the validity of the adopted modeling approach.

3- The results and discussion

This section examines the structural responses to column removal scenarios, focusing on damage percentage index (DPI), ductility demand criteria, i.e. rotational demand over yield rotation, and the vertical displacement of the node above the removed column.

Given that corner column removals resulted in more critical situations, the related findings are outlined below.

3-1- Damage percentage index (DPI)

To assess the collapse potential of structures, an index called hereafter the damage percentage index (DPI) is defined in Eq. (4):

$$DPI = \frac{n_i}{n_t} \tag{4}$$

Where, n_i is the of the number of collapses of the desired column removal scenario (in the i^{th} floor), and n_t is the total number of column removal scenarios. Given that either a middle or a corner column is removed, overall, in the 5-story, the 10-story, and the 15-story buildings, 10, 20, and 30 scenarios are assumed, respectively. In general, 340 column removal scenarios were considered. The results are shown in Table 3.

Table 3: DP for the case studies

Case studied	The story number where failure occurs		%DPI
	Middle column	Corner column	
5S.3B.6BL.8R.HER	-	-	-
5S.3B.6BL.8R.HER.WSC.WB	-	-	-
5S.3B.6BL.4.5R.HER	-	5	10

5S.3B.6BL.4.5R.MER	-	5	10
5S.3B.6BL.8R.MER	4,5	4,5	40
5S.3B.6BL.8R.MER.WSC.WB	4,5	4,5	40
5S.3B.6BL.4.5R.LER	3,4,5	3,4,5	60
5S.3B.6BL.8R.LER	3,4,5	3,4,5	60
10S.3B.6BL.8R.HER	-	10	5
10S.3B.6BL.8R.HER.WSC.WB	-	10	5
10S.3B.6BL.4.5R.HER	-	10	5
10S.3B.6BL.4.5R.MER	10	10	10
10S.3B.6BL.8R.MER	-	10	5
10S.3B.6BL.8R.MER.WSC.WB	-	10	5
10S.3B.6BL.4.5R.LER	7,8,9,10	7,8,9,10	40
15S.3B.6BL.8R.HER	-	-	-
15S.3B.6BL.8R.HER.WSC.WB	-	-	-
15S.3B.6BL.8R.MER	-	15	3.33
15S.3B.6BL.8R.MER.WSC.WB	-	15	3.33

Based on the results in Table 3., the structures located in the low seismicity have the highest DPI which shows that they are considerably vulnerable under column removal cases, regardless of their lateral-resisting ductility level.).

The DPI reached 60% for both 5S.3B.6BL.4.5R.LER and 5S.3B.6BL.8R.LER cases, indicating a high vulnerability to progressive collapse regardless of the ductility level of the lateral-resisting system. In 5-story buildings located in high seismicity regions, special moment frames (SMFs) exhibited marginally better performance than intermediate moment frames (IMFs), with no collapse observed (DPI = 0). However, under medium seismicity conditions, SMFs showed significantly higher DPI values (DPI = 40%), approximately four times greater than those of IMFs.

This trend suggests that, in low-rise structures designed for moderate seismicity, the increased ductility associated with SMFs does not necessarily translate into improved progressive collapse resistance, likely due to the use of smaller member sizes associated with higher R factors. Consequently, in cases where code limitations do not restrict their application, IMFs may provide more favorable performance in terms of progressive collapse resistance when evaluated using the DPI criterion.

For 10-story buildings in moderate seismicity, SMFs were also more robust than IMFs, though to a lower DPI than in the 5-story case. In medium seismicity, varying ductility levels exacerbate structural damage

sensitivity. Lower seismicity design levels generally lead to increased DPI (up to 40%), making structures more vulnerable to collapse due to weaker bearing elements. Additionally, results show that considering the SC. WB principle doesn't affect the DPI

Furthermore, the results indicate that the 15-story frames exhibit greater robustness compared to the lower-rise structures, as the special moment frames show the lowest DPI values, reaching approximately 3.33% in the most critical cases. In general, an increase in building height is associated with a reduction in DPI, which can be attributed to the greater number of structural elements available for load redistribution following column removal.

Overall, based on the DPI criterion, special moment frames (SMFs) tend to exhibit lower collapse potential than intermediate moment frames (IMFs), with the exception of case 5S.3B.6BL.8R.MER. However, at low seismicity levels, the ductility level of the lateral-resisting system does not appear to significantly influence the progressive collapse response. Considering that ASCE 7 imposes height limitations on the use of IMFs in higher seismic design categories, and in light of the DPI results, SMFs can generally be considered more reliable options for mid- and high-rise structures.

The DPI results also provide useful insight for identifying critical regions requiring retrofit. For structures designed for low seismicity levels, column removal in the upper three and four stories led to collapse in low- and mid-rise buildings, respectively. In contrast, for other cases, collapse was primarily triggered by column removal in the upper two stories. These findings suggest that strengthening of beams and columns should be prioritized in these critical story levels to enhance progressive collapse resistance.

3-2- Ductility demand

The ductility demand (μ) was defined in Eq. (5):

$$\mu = \frac{\theta_u}{\theta_y} \tag{5}$$

Where, θ_u is the rotational demand, and θ_y is the yield rotation of the beam. The amounts of ductility demands are shown in Table 4. It is worth mentioning that based on the UFC limit states and performance levels in the ASCE41-23, all of the ductility demands are less than the acceptance criteria, which shows that the RBS connections are resistant to progressive collapse. Based on the results, the buildings with low seismicity have passed the IO limitation (with ductility demand more than 5). Also, the structures in the medium seismicity had amplified considerably the plastic rotations of those in the high seismicity. All of the case studies in the high seismicity even did not experience the yielding under column removal scenarios which shows that conservative design parameters of seismic regulation make them resistant to progressive collapse. Notably, frame ductility levels significantly affected ductility demands at lower seismicity levels. At high seismicity, structures are designed for larger seismic forces (based on forced-based regulations), resulting in sufficient robustness and reduced sensitivity of ductility demands to frame ductility level changes. These structures also show ductility demands of less than 1. Ignoring the SC. WB principle, however, doesn't change the performance level but amplifies the ductility demand up to 1.83 times. Amplification was greater in the 10-story models. Although high-rise and mid-rise buildings are generally more robust than low-rise buildings due to their additional elements for force redistribution. after a column is removed, the SC.WB principle plays a more crucial role in these structures.

Table 4: Comparison of progressive collapse ductility demands of the case studied

Case studied	Performance level of plastic hinges	Maximum Ductility demand
5S.3B.6BL.8R.HER.RBS	IO	0.087
5S.3B.6BL.8R.HER.WSC.WB	IO	0.087
5S.3B.6BL.4.5R.HER	IO	0.084
5S.3B.6BL.4.5R.MER	IO	0.52
5S.3B.6BL.8R.MER	IO	2.24
5S.3B.6BL.8R.MER.WSC.WB	IO	2.84
5S.3B.6BL.4.5R.LER	IO-LS	5.23
5S.3B.6BL.8R.LER	IO-LS	5.85
10S.3B.6BL.8R.HER	IO	0.12
10S.3B.6BL.8R.HER.WSC.WB	IO	0.22
10S.3B.6BL.4.5R.HER	IO	0.081
10S.3B.6BL.4.5R.MER	IO-LS	4.05
10S.3B.6BL.4.5R.LER	IO-LS	6.67

10S.3B.6BL.8R.MER	IO	0.55
10S.3B.6BL.8R.MER.WSC.WB	IO	0.98
15S.3B.6BL.8R.HER	IO	0.071
15S.3B.6BL.8R.HER.WSC.WB	IO	0.080
15S.3B.6BL.8R.MER	IO	0.1
15S.3B.6BL.8R.MER.WSC.WB	IO	0.15

In 5-story buildings, IMFs exhibited lower ductility demands than SMFs due to their larger beams. However, in 10-story buildings, the ductility demand comparison was seismicity-dependent. At medium seismicity, IMFs showed considerably higher demands than SMFs, whereas at high seismicity, IMFs had lower demands. It seems to neglect the seismic design criterion of ASCE7 resulting in more sensitivity in the medium seismicity case, Even the 10-story SMF without the SC.WB principle had lower ductility demand than the IMF.

In the 15-story buildings, RBS connections exhibited the lowest ductility demands, with all cases remaining within the Immediate Occupancy (IO) performance level. At high seismicity levels, neglecting the strong column–weak beam (SC–WB) principle resulted in only a marginal increase in ductility demand (approximately 12%) compared to the corresponding baseline structures. However, under moderate seismicity conditions, the effect became more pronounced, with ductility demand increasing by approximately 50% when the SC–WB principle was not satisfied.

Furthermore, a general trend was observed in which ductility demand increased as the seismicity level decreased, with increases of approximately 40% and 87.5% for structures satisfying and violating the SC–WB principle, respectively. Notably, in all special moment frames designed for medium and high seismicity levels, the connections remained within the IO performance level even under the most critical column removal scenarios. This indicates that the incorporation of RBS connections in special moment frames provides adequate robustness against progressive collapse in tall buildings.

3-3-Vertical displacement

In Figs. 8(a) to 8(c), the vertical displacement time histories for the node above the removed column in the most critical cases of the 5-story, 10-story, and 15-story structures, are shown respectively. In the 5-story structures, the scenario without the SC.WB principle exhibited the largest vertical displacement. However, in the 10-story structures, the IMF case under medium seismicity level resulted in the most significant vertical displacement. In all structures, disregarding the SC.WB principle at moderate seismicity levels led to a significant change in displacement.

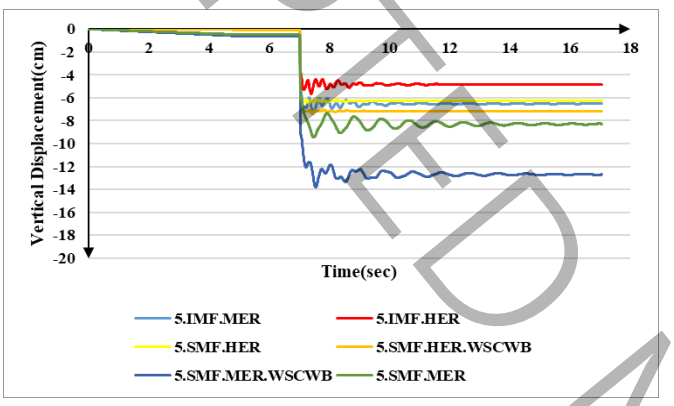

(a) 5-story buildings

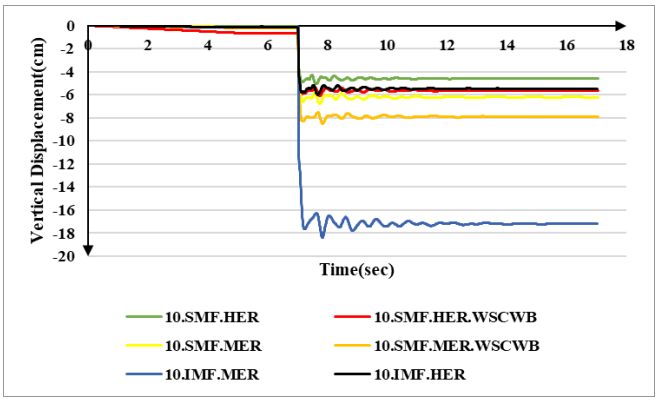

(b) 10-story buildings

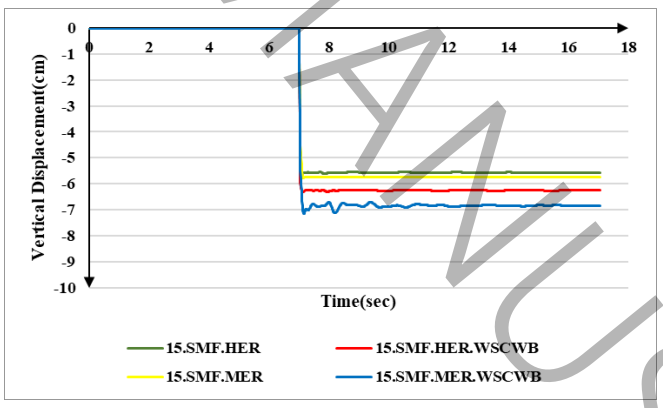

(c) 15-story buildings

Fig. 8: Time history of vertical nodal displacements

Fig. 9 shows the maximum vertical displacements of the node above the removed column for various case studies. Buildings located in areas with low seismicity display the highest displacements. The vertical displacement generally ranged between 5 and 8 cm for most cases. However, frames designed for low seismicity levels exhibited significantly larger displacements, ranging from 15 to 22 cm, which are

approximately three to four times greater than those observed in frames designed for medium and high seismicity levels. When the SC.WB principle is not taken into account, displacements tend to increase, particularly in lower seismicity levels. For example, in the case of 5S.3B.6BL.8R.MER, ignoring this principle resulted in the response being amplified by 1.56 times. All structures designed for the high seismicity showed vertical displacements lower than 7cm, regardless of their ductility levels. For the 15-story buildings, all vertical nodal displacements remained below 7 cm under both medium and high seismicity conditions. Neglecting the strong column–weak beam (SC–WB) principle led to an increase in vertical displacement of approximately 22% in these structures. In addition, variations in seismicity level did not result in significant changes in the displacement response of the tall buildings.

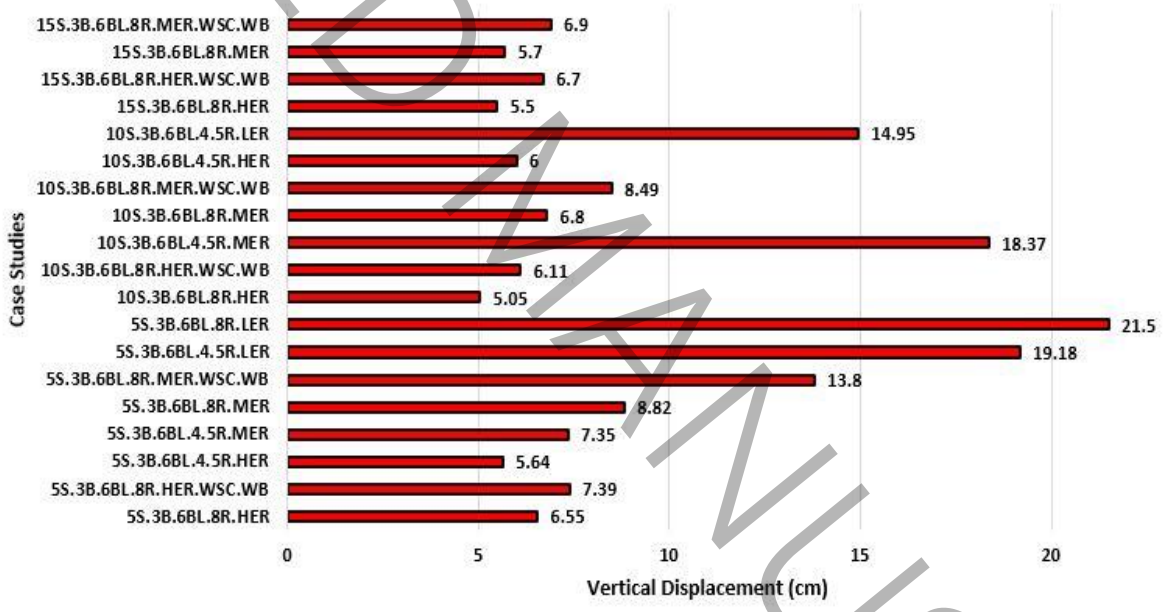

Fig. 9: The maximum amount of vertical nodal displacements

The locations of the floors where column removal caused the most significant vertical displacements are summarized in Table D1 in Appendix D. In all instances, the maximum displacements occurred on the floor directly below the story where the failure happened (the floors with the highest DPI, had the largest vertical nodal displacements). However, in the case of 5S.3B.6BL.8R.LER, the maximum vertical displacement was observed in the story where the failure occurred. Therefore, if retrofitting is necessary, it is advisable to renovate the structural elements from the floor beneath the story where the failure occurs to the last story.

4-Sensetivity assessment

In the design of structures, designers must consider scenarios that comply with design codes. However, when addressing special design situations such as progressive collapse, the potential for damage increases, but this issue is not considered in the design regulation. Therefore, it is essential to evaluate which design parameters can effectively ensure adequate robustness in the structure, especially in the performance-based approaches. This issue becomes more determinative in the structures in the medium and high seismicity areas, where the structures have the least strength against column removal scenarios, and it is hard to decide to choose a ductility level for the specified seismicity of the area. To evaluate the impact of varying each seismic parameter on the structural robustness, the maximum changes in controlling parameters (acceptance criteria) including the ductility demand, and vertical nodal displacement, were assessed in the specified seismicity. This index quantifies the sensitivity of a structure's response to changes in design variables. The maximum increase index is not evaluated for structures in low seismicity areas because they lack sufficient robustness and require specialized retrofitting for progressive collapse prevention, regardless of their lateral-resisting system.

Figs. 10(a) and 10(b) illustrate the maximum increase in ductility demands. Structures in medium seismicity are more sensitive to changes in ductility demand and the ductility level of lateral-resisting system is the controlling parameter in the response amplification. Given that variations in seismicity level can significantly influence sensitivity assessments, the effects of ductility level and the strong column–weak beam (SC–WB) principle were specifically evaluated under medium (MER) and high (HER) seismicity conditions.

For the 15-story buildings, only special moment frames were considered as the lateral-resisting system; therefore, the ductility level was not treated as a variable parameter. However, the influence of the SC–WB principle remained significant. The ratio of ductility demand in structures without the SC–WB requirement

to that of the corresponding baseline structures was approximately 1.13 and 1.50 under high and medium seismicity levels, respectively.

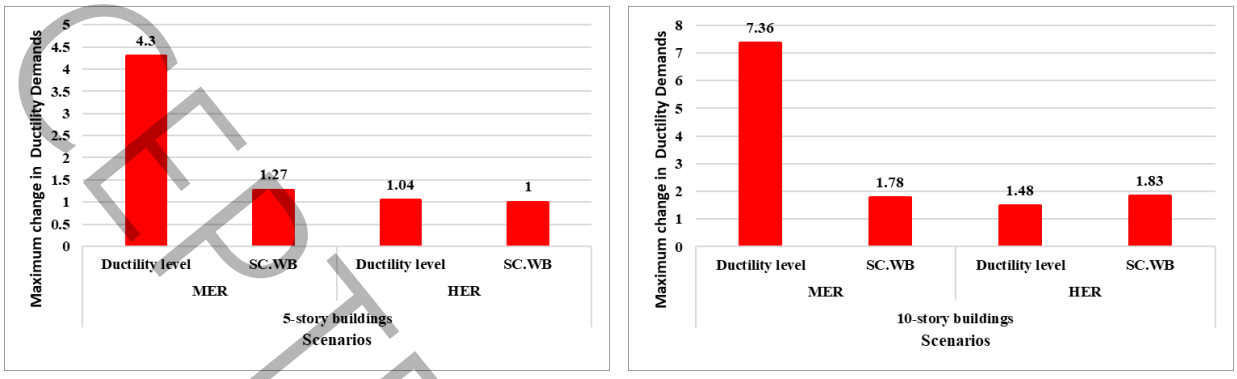

(a) 5-story buildings (b) 10-story buildings

Fig. 10: The maximum increase in the ductility demands

Furthermore, Figs. 11(a) and 11(b) illustrate the maximum increase in vertical displacement above the removed column. The results indicate that there is not a significant change in vertical displacements for case studies in high seismicity areas. However, the parameters of SC.WB and ductility level lead to considerable changes in medium seismicity areas. It can also be concluded that in most case studies within medium seismicity areas, the ductility level of frames is a critical factor that contributes to higher ductility demands and vertical displacements. The SC.WB principle is particularly effective in amplifying ductility demands, especially in 10-story buildings. For the 15-story cases, the vertical displacement got 1.21 times larger, when the SC.WB principle was neglected.

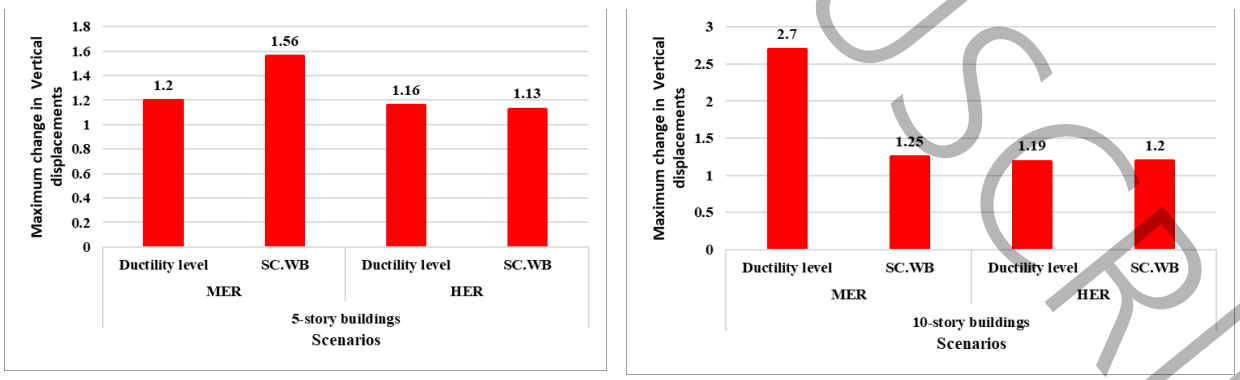

(c) 5-story buildings (d) 10-story buildings

Fig. 11: The maximum increase in the vertical nodal displacements

By considering the combined effects of the damage percentage index (DPI), vertical displacement, and ductility demand, distinct trends can be identified the structures. For low-rise buildings, the results indicate that under medium seismicity conditions, intermediate moment frames (IMFs) may provide more favorable performance. Under high seismicity, however, the differences between special moment frames (SMFs) and IMFs become negligible across all evaluated criteria, suggesting that economic considerations may govern the selection of the lateral-resisting system.

In contrast, a different trend is observed for taller structures. In these cases, the response parameters show more pronounced sensitivity, and code-imposed limitations on the use of IMFs (e.g., height restrictions in ASCE 7) become more critical. Consequently, SMFs can be considered more appropriate for mid- and high-rise buildings, both from a performance and code-compliance perspective. This aspect has not been sufficiently addressed in some previous studies and may lead to misleading conclusions, particularly for structures with lower inherent robustness.

Previous studies [23,24] have identified mid-rise frames as more vulnerable to progressive collapse. In addition, some studies [4] have reported that RBS connections may lead to increased plastic rotations and vertical displacements in low-rise frames. However, the present results show that when RBS connections are implemented in special moment frames designed for higher seismicity levels, their influence on ductility demand and vertical displacement is not significant (e.g., SMF(8R).HER cases).

Therefore, for reliable progressive collapse-resistant design, it is essential to consider the combined effects of ductility demand, building height, connection type, and seismic design provisions. A balanced and context-dependent selection of these parameters is necessary to avoid excessive structural sensitivity and to ensure adequate robustness under column removal scenarios.

5- Conclusion

This study examines the progressive collapse behavior of steel moment frame structures with RBS connections under various column removal scenarios. 19 structures were evaluated using nonlinear

dynamic analysis, taking into account various seismic parameters, including story number, seismicity level, the ductility level of the lateral-resisting system, and the strong column-weak beam philosophy. The nonlinear evaluation was performed using the OpenSees software and involved the lumped plasticity model. To assess the collapse behavior of the structures, DPI and vertical nodal displacement were analyzed. Additionally, conventional acceptance criteria, such as ductility demands, were checked according to the UFC and ASCE 41-23 standards. The following results were obtained from this study:

- Designing structures for lower seismicity levels has increased DPI. Case studies indicated that buildings with higher DPI experienced greater ductility demands and vertical nodal displacements. Specifically, scenarios where DPI exceeded 60% for 5-story buildings and 40% for 10-story buildings were identified as the most critical. Furthermore, in these cases, alteration in the ductility level of the lateral-resisting system did not significantly affect the results. Therefore, employing highly ductile structural systems or connections is not effective in reducing the potential for collapse in these frames and special retrofitting is necessary to achieve acceptable levels of robustness. In these scenarios, connections such as WUF-W, Side plate, and strengthening methods (cover plates, haunches, and etc.) can be more applicable.
- The RBS connections under the worst scenario (ductility demand=6.67) demonstrated an IO-LS performance level that met the acceptance criteria of the regulations, indicating these connections are generally resistant to progressive collapse, regardless of seismic design considerations. In the other words, in the previous studies, RBS connections were known as robust connections based on their catenary action and axial resistance. In this study, the behavior of the connections was represented using a moment–rotation backbone within a lumped plasticity framework. The results indicate that the observed hinge performance levels are consistent with findings from previous studies and support the classification of RBS connections as robust against progressive collapse. At the same time, the results highlight that other design parameters can significantly influence the magnitude of structural demands.

- Ignoring the strong column-weak beam principle in special moment frames did not increase the DPI. However, in the most unfavorable scenarios, it amplified the ductility demand and vertical displacement by 1.83 and 1.56 times greater, respectively, compared to structures that adhered to this principle. Consequently, this principle can significantly impact the structural robustness, particularly in sensitive (lower seismicity) structures.
- Among 10-story buildings, SMF structures are preferred over IMF structures because generally they exhibit lower DPI, ductility demands, and vertical displacements, especially under medium seismic conditions. Although IMF structures in high seismic zones show slightly lower ductility demands than SMF structures, the ASCE 7 guidelines impose a height limitation of 20 meters for IMF cases in seismic design category D. As a result, SMF buildings are generally considered more reliable and also acceptable choices for high-rise and mid-rise structures. In addition, the 10S.3B.6BL.4.5R.MER case exhibited relatively high response demands, with a ductility demand of 4.04, vertical displacement of 18.4 cm, and a notable DPI value. Considering these results, together with the height limitations imposed by ASCE 7 on the use of intermediate moment frames, it is recommended that specific retrofitting strategies be considered for existing mid- and high-rise IMF structures to enhance their resistance to progressive collapse.
- In the low-rise frames, ASCE7 permits the use of IMF and SMF structures, so choosing the ductility level of frames is more challenging. In the structures located in high, the lateral-resisting frame's ductility level did not have a huge effect on the results. Although SMF structures demonstrated lower DPI (under considering the strong column-weak principle), some IMF structures showed less ductility demands and vertical displacements. In moderate seismicity, IMF cases outperformed SMF cases across all parameters. Thus, for low-rise frames in moderate seismic conditions, high ductility levels and design considerations are unnecessary, making IMFs a preferable option for designers. In such cases, economic and practical considerations may become more influential than purely technical parameters. Accordingly, the adoption of RBS connections may not necessarily lead to a significant improvement in structural robustness and should be evaluated in the context of

overall design objectives. Modifying the ductility level and SC.WB parameters resulted in significant changes to the structural responses. However, in most cases, the ductility level of the lateral-resisting system was more critical, particularly in medium seismicity areas, where structures had weaker components. Therefore, it is advisable to evaluate various design scenarios for sensitive structures to ensure that the frames have an appropriate ductility level and sufficient strength to withstand progressive collapse.

- In high-rise buildings, the 15-story special moment frames exhibited the lowest ductility demands (0.071 and 0.10 for the HER and MER cases, respectively) compared to the corresponding 5- and 10-story frames. In addition, the maximum DPI in these structures was limited to 3.33%, representing the lowest value among all cases, while vertical displacements remained below 10 cm. These results indicate that, in tall buildings, RBS connections do not lead to excessive demand concentrations and can provide adequate robustness against progressive collapse. In this study, RBS connections were modeled using a lumped plasticity approach with concentrated hinges to evaluate hinge performance and the overall structural response.
- While this modeling framework is effective for assessing deformation demands, identifying critical response regions, and supporting retrofit-oriented evaluations, it does not explicitly capture catenary action or the axial resistance of connections. In addition, interaction effects between axial force and bending are not directly represented, which may influence the response, particularly in taller structures. Furthermore, the lumped plasticity approach does not explicitly model the spatial distribution of yielding or potential fracture locations, which may affect the accuracy of local response predictions. The analyses were also performed using two-dimensional models, which, although commonly adopted in previous studies [23], may lead to conservative estimates of ductility demand, vertical displacement, and collapse indicators due to limited representation of three-dimensional load redistribution mechanisms. In addition, the contribution of panel zone deformation was not considered in the present study, although it can influence connection behavior and overall system response, particularly in cases with lower structural robustness. Therefore,

future studies are recommended to incorporate three-dimensional modeling, explicit simulation of connection axial behavior, and panel zone effects to provide a more comprehensive assessment of progressive collapse resistance.

6- References

[1] V. Gioncu, and Mazzolani, F., Seismic Design of Steel Structures,Boca Raton,FL: CRC Press., 2013.

[2] M. Bruneau, Chi-Ming Uang, Sabelli, R., Ductile Design of Steel Structures, 2 ed., McGraw Hill, 2011.

[3] E. Brunesi, R. Nascimbene, G. Rassati, Seismic response of MRFs with partially-restrained bolted beam-to-column connections through FE analyses, Journal of Constructional Steel Research, 107 (2015) 37-49.

[4] T. Kim, J. Kim, Collapse analysis of steel moment frames with various seismic connections, Journal of Constructional Steel Research, 65(6) (2009) 1316-1322.

[5] E.P. Popov, T.-S. Yang, S.-P. Chang, Design of steel MRF connections before and after 1994 Northridge earthquake, Engineering Structures, 20(12) (1998) 1030-1038.

[6] C. Sofias, C. Kalfas, D. Pachoumis, Experimental and FEM analysis of reduced beam section moment endplate connections under cyclic loading, Engineering Structures, 59 (2014) 320-329.

[7] F. Kiakojouri, V. De Biagi, B. Chiaia, M.R. Sheidaii, Progressive collapse of framed building structures: Current knowledge and future prospects, Engineering Structures, 206 (2020) 110061.

[8] F. Hashemi Rezvani, B. Behnam, H. Reza Ronagh, M.S. Alam, Failure progression resistance of a generic steel moment-resisting frame under beam-removal scenarios, International Journal of Structural Integrity, 8(3) (2017) 308-325.

[9] B. Behnam, F.H. Rezvani, Structural Evaluation of Tall Steel Moment-Resisting Structures in Simulated Horizontally Traveling Postearthquake Fire, Journal of Performance of Constructed Facilities, 30(2) (2016) 04014207.

[10] GSA, Progressive collapse analysis and design guidelines for new federal office buildings and major modernization projects, in, General Services Administration, Washington (DC), 2003.

[11] UFC, Design of buildings to resist progressive collapse, in, Unified Facilities Criteria, Washington (DC), 2009.

[12] J. Park, J. Kim, Fragility analysis of steel moment frames with various seismic connections subjected to sudden loss of a column, Engineering Structures, 32(6) (2010) 1547-1555.

[13] F. McKenna, OpenSees: a framework for earthquake engineering simulation, Computing in Science & Engineering, 13(4) (2011) 58-66.

[14] K. Khandelwal, S. El-Tawil, Pushdown resistance as a measure of robustness in progressive collapse analysis, Engineering Structures, 33(9) (2011) 2653-2661.

[15] A. Hadidi, R. Jasour, A. Rafiee, On the progressive collapse resistant optimal seismic design of steel frames, Structural engineering and mechanics: An international journal, 60(5) (2016) 761-779.

[16] I. Faridmehr, M.H. Osman, M.B.M. Tahir, A.F. Nejad, R. Hodjati, Seismic and progressive collapse assessment of SidePlate moment connection system, Structural Engineering and Mechanics, 54(1) (2015) 35-54.

[17] S.-Y. Lee, S.-Y. Noh, D. Lee, Evaluation of progressive collapse resistance of steel moment frames designed with different connection details using energy-based approximate analysis, Sustainability, 10(10) (2018) 3797.

[18] S.-Y. Lee, S.-Y. Noh, D. Lee, Comparison of progressive collapse resistance capacities of steel ordinary and intermediate moment frames considering different connection details, Engineering Structures, 231 (2021) 111753.
[19] C. Chen, H. Qiao, J. Wang, Y. Chen, Progressive collapse behavior of joints in steel moment frames involving reduced beam section, Engineering Structures, 225 (2020) 111297.
[20] F. Dinu, I. Marginean, D. Dubina, Experimental testing and numerical modelling of steel moment-frame connections under column loss, Engineering Structures, 151 (2017) 861-878.
[21] K. Qian, X. Lan, Z. Li, Y. Li, F. Fu, Progressive collapse resistance of two-storey seismic configured steel sub-frames using welded connections, Journal of Constructional Steel Research, 170 (2020) 106117.
[22] B. Meng, W. Zhong, J. Hao, X. Song, Improving anti-collapse performance of steel frame with RBS connection, Journal of Constructional Steel Research, 170 (2020) 106119.
[23] H. Semsarha, P. Tehrani, B. Behnam, A Comparative Study on Pre-and Post-Earthquake Progressive Collapse Resistance of 2D and 3D Steel Structures, International Journal of Civil Engineering, 21(7) (2023) 1141-1157.
[24] H. Semsarha, P. Tehrani, B. Behnam, Post-earthquake progressive failure resistance of steel frames under column-removal scenarios, in: Structures, Elsevier, 2021, pp. 1544-1560.
[25] W. Zhang, Z. Xu, H. Xu, W. Zhang, Z. Wang, Y. Chen, Post-fire progressive collapse resistance of beam-column substructures with RBS connections, Journal of Constructional Steel Research, 224 (2025) 109137.
[26] I. Faridmehr, M.H. Osman, M.M. Tahir, A.F. Nejad, M. Azimi, Seismic and progressive collapse assessment of new proposed steel connection, Advances in Structural Engineering, 18(3) (2015) 439-452.
[27] B. Behnam, F. Shojaei, H.R. Ronagh, Seismic progressive-failure analysis of tall steel structures under beam-removal scenarios, Frontiers of Structural and Civil Engineering, 13 (2019) 904-917.
[28] F. Wang, J. Yang, Z. Pan, Progressive collapse behaviour of steel framed substructures with various beam-column connections, Engineering Failure Analysis, 109 (2020) 104399.
[29] B. Rezaee, P. Tehrani, B. Behnam, Post-earthquake progressive collapse behavior of steel frames with reduced beam section connections, Structural Engineering and Mechanics, 97 (2026) 505-533.
[30] ASCE, Minimum design loads, and associated criteria for buildings and other structures, ASCE/SEI Standrad 7-16, in, American Society of Civil Engineers, Reston, Virginia, 2016.

[31] AISC, Specification for Structural Steel Buildings, Standard ANSI/AISC 360-16, in, American Institute of Steel Construction,Chicago, Illinois, 2016.

[32] AISC, Seismic Provisions for Structural Steel Buildings, ANSI/AISC Standard 341-16, in, American Institute of Steel Construction Chicago, Illinois 2016.

[33] AISC, Prequalified Connections for Special and Intermediate Steel Moment Frames for Seismic Applications, Standard ANSI/AISC 358-16, in, American Institute of Steel Construction, Chicago, Illinois, 2016.
[34] J. Kim, T. Kim, Assessment of progressive collapse-resisting capacity of steel moment frames, Journal of Constructional Steel Research, 65(1) (2009) 169-179.
[35] ASCE, Seismic Evaluation and Retrofit of Existing Buildings, ASCE/SEI Standard 41-23, in, American Society of Civil Engineers, Reston, Virginia, 2023.
[36] D.G. Lignos, H. Krawinkler, Deterioration Modeling of Steel Components in Support of Collapse Prediction of Steel Moment Frames under Earthquake Loading, Journal of Structural Engineering, 137(11) (2011) 1291-1302.
[37] NIST, Guidelines for Nonlinear Structural Analysis for Design of Buildings: Part IIa – Steel Moment Frames, GCR 17-917-46v2, Applied Technology Council, Redwood, California, 2017.
[38] F. Zareian, R.A. Medina, A practical method for proper modeling of structural damping in inelastic plane structural systems, Computers & structures, 88(1-2) (2010) 45-53.

[39] A.K. Chopra, Dynamics of structures, Pearson Education India, 2007.
[40] D.G. Lignos, J. Cravero, A. Elkady, Experimental Investigation of the Hysteretic Behavior of Wide-Flange Steel Columns under High Axial Load and Lateral Drift Demands, in, 2016.
[41] D. Lignos, A.R. Hartloper, A.M.A. Elkady, R. Hamburger, G. Deierlein, Revised ASCE-41 modeling recommendations for moment-resisting frame systems, in: Proceedings of the 11th US National Conference on Earthquake Engineering (11NCEE), 2018.

Appendix A

Nonlinear modeling parameters and acceptance criteria are detailed in Table A1. The acceptance criterion for the Life Safety (LS) level in ASCE41-23 is similar to that in the UFC, though the UFC criterion is slightly more conservative.

Table A1: The acceptance criteria in the RBS connections [11, 35]

ASCE41-23[35]						
RBS	Nonlinear modeling parameters			Acceptance criteria		
	a-plastic rotation	b-plastic rotation	c-residual strength	IO	LS	CP
	0.05-0.0003d	0.07-0.0003d	0.2	-0.025 0.00015d	-0.0525 0.00023d	0.07-0.0003d
UFC						
Nonlinear modeling parameters				Acceptance criteria		
RBS	a-plastic rotation	b-plastic rotation	c-residual strength	Primary	Secondary	
	0.05-0.0003d	0.07-0.0003d	0.2	0.05-0.0003d	0.07-0.0003d	

Appendix B

The cross sections of the structures are described below.

Table B1: cross sections of the 15-story cases

Cases	15S.3B.6BL.8R.HER		15S.3B.6BL.8R.HER.WSC.WB	
story	columns	beams	columns	beams
1	BOX500X35	W21X62	BOX450X35	W21X62
2	BOX450X35	W21X62	BOX400X35	W21X62
3	BOX450X35	W21X62	BOX400X35	W21X62
4	BOX450X35	W21X62	BOX400X35	W21X62

5	BOX450X35	W21X50	BOX400X35	W21X50
6	BOX450X35	W21X50	BOX400X35	W21X50
7	BOX400X35	W21X50	BOX340X35	W21X50
8	BOX400X35	W21X50	BOX340X35	W21X50
9	BOX400X35	W18X40	BOX340X35	W18x40
10	BOX400X35	W16X77	BOX320X30	W16x77
11	BOX350X35	W16X77	BOX300X30	W16x77
12	BOX350X35	W16X77	BOX300X30	W16x77
13	BOX350X35	W16X77	BOX300X30	W16x77
14	BOX350X35	W16X77	BOX300X30	W16x77
15	BOX350X35	W16X77	BOX260X20	W16x77
Cases	15S.3B.6BL.8R.MER		15S.3B.6BL.8R.MER.WSC.WB	
story	columns	beams	columns	beams
1	BOX450X35	W21X55	BOX400X35	W21X55
2	BOX450X35	W21X55	BOX400X35	W21X55
3	BOX450X35	W21X55	BOX400X35	W21X55
4	BOX400X35	W21X55	BOX340X35	W21X55
5	BOX400X35	W21X50	BOX340X35	W21X50
6	BOX400X30	W16X67	BOX340X35	W16X67
7	BOX340X35	W16X67	BOX260X20	W16X67
8	BOX340X35	W16X67	BOX260X20	W16X67
9	BOX340X35	W16X67	BOX260X20	W16X67
10	BOX340X35	W16X50	BOX260X20	W16X50
11	BOX300X30	W16X50	BOX260X20	W16X50
12	BOX300X30	W16X50	BOX260X20	W16X50
13	BOX300X30	W16X50	BOX20X30	W16X50
14	BOX260X20	W16X50	BOX20X30	W16X50
15	BOX260X20	W16X50	BOX20X30	W16X50

Table B2: cross sections of the 10-story cases

Cases	10S.3B.6BL.8R.HER		10S.3B.6BL.8R.HER.WSC.WB		10S.3B.6BL.4.5R.MER	
story	columns	beams	columns	beams	columns	beams
1	BOX450X35	W21X62	BOX340X35	W21X62	BOX400X35	W21X62
2	BOX450X35	W21X62	BOX340X35	W21X62	BOX340X30	W21X62
3	BOX450X35	W21X62	BOX300X30	W21X62	BOX340X30	W21X62
4	BOX400X35	W21X62	BOX300X30	W21X62	BOX300X30	W21X62
5	BOX400X35	W21X62	BOX300X30	W21X62	BOX300X30	W21X55
6	BOX400X35	W21X62	BOX300X30	W21X62	BOX300X30	W21X55
7	BOX400X35	W21X50	BOX300X30	W21X50	BOX300X30	W21X55
8	BOX400X35	W21X50	BOX300X30	W21X50	BOX260X20	W18X40
9	BOX300X30	W18x40	BOX260X20	W18x40	BOX260X20	W18X40

10	BOX300X30	W18x40	BOX260X20	W18x40	BOX180X20	W14X26
Cases	10S.3B.6BL.8R.MER		10S.3B.6BL.8R.MER.WSC.WB		10S.3B.6BL.4.5R.LER	
story	columns	beams	columns	beams	columns	beams
1	BOX400X35	W21X50	BOX320X30	W21X50	BOX320X30	W18X40
2	BOX400X35	W21X50	BOX300X30	W21X50	BOX300X30	W18X40
3	BOX400X35	W21X50	BOX300X30	W21X50	BOX300X30	W18X40
4	BOX400X35	W21X50	BOX300X30	W21X50	BOX300X30	W18X40
5	BOX400X35	W21X50	BOX300X30	W21X50	BOX300X30	W18X40
6	BOX300X30	W21X50	BOX300X30	W21X50	BOX260X20	W18X40
7	BOX300X30	W18X40	BOX260X20	W18X40	BOX260X20	W16X36
8	BOX300X30	W18X40	BOX260X20	W18X40	BOX260X20	W16X36
9	BOX300X30	W18X40	BOX260X20	W18X40	BOX180X20	W16X36
10	BOX260X30	W16X31	BOX260X20	W16X31	BOX180X20	W14X22

Table B3: cross sections of the 5-story cases

Cases	5S.3B.6BL.8R.HER		5S.3B.6BL.4.5R.HER		5S.3B.6BL.4.5R.MER		5S.3B.6BL.8R.MER	
story	columns	beams	columns	beams	columns	beams	columns	beams
1	BOX380x40	W21X50	BOX340x35	W16X77	BOX300X30	W14X68	BOX340X30	W14X26
2	BOX380X40	W21X50	BOX340X35	W16X77	BOX300X30	W14X68	BOX340X30	W18X40
3	BOX380X40	W21X50	BOX300X30	W16X67	BOX300X30	W14X61	BOX300X30	W18X40
4	BOX300X35	W21X44	BOX300X30	W16X67	BOX260X20	W14X48	BOX300X30	W16X31
5	BOX300X35	W21X44	BOX260X20	W16X31	BOX260X20	W14X48	BOX260X20	W14X26
Cases	5S.3B.6BL.4.5R.LER		5S.3B.6BL.8R.HER.WSCWB		5S.3B.6BL.8R.MER.WSCWB		5S.3B.6BL.8R.LER	
story	columns	beams	columns	beams	columns	beams	columns	beams
1	BOX260X20	W14X48	BOX300x30	W21X50	BOX300x30	W14X26	BOX300X30	W16X31
2	BOX260X20	W14X48	BOX300X30	W21X50	BOX300X30	W18X40	BOX300X30	W16X31
3	BOX200X25	W14X43	BOX260X20	W21X50	BOX260X20	W18X40	BOX300X30	W16X31
4	BOX200X25	W14X43	BOX260X20	W21X44	BOX260X20	W16X31	BOX300X30	W14X43
5	BOX200X25	W12X26	BOX260X20	W21X44	BOX260X20	W14X26	BOX260X20	W14X26

Appendix C

The geometric properties of RBS connections are described below.

Table C1: The geometric characteristics of the RBS connections

Sections	bbf(cm)	db(cm)	a(cm)	b(cm)	c(cm)	Sh-(a+b/2)(cm)
W12X26	16.50	31.00	9.90	21.70	4.13	20.75

W14X22	12.70	34.80	7.62	24.36	3.18	19.80
W14X26	12.77	35.30	7.66	24.71	3.19	20.02
W14X43	20.32	34.80	12.19	24.36	5.08	24.37
W14X48	20.40	35.00	12.24	24.50	5.10	24.49
W14X61	25.4	35.3	15.24	24.71	6.35	27.60
W14X68	25.4	35.53	15.24	24.87	6.35	27.68
W16X31	14.46	40.40	8.68	28.28	3.62	22.82
W16X36	17.75	40.36	10.65	28.25	4.44	24.78
W16X67	25.90	41.40	15.54	28.98	6.48	30.03
w16x77	26.16	41.90	15.70	29.33	6.54	30.36
W18X40	15.29	45.50	9.17	31.85	3.82	25.10
W21X44	16.50	52.30	9.90	36.61	4.13	28.21
W21x50	16.60	52.80	9.96	36.96	4.15	28.44
W21X55	20.90	52.80	12.54	36.96	5.23	31.02
W21X62	20.93	53.34	12.56	37.34	5.23	31.23
W21X73	21.00	53.40	12.60	37.38	5.25	31.29

Appendix D

The location of floors with the maximum response are provided.

Table D1: The location of the floor with the maximum vertical displacement

Cases	Floor with the maximum displacement
5S.3B.6BL.8R.HER	5
5S.3B.6BL.8R.HER.WSC.WB	5
5S.3B.6BL.4.5R.HER	4
5S.3B.6BL.4.5R.MER	4
5S.3B.6BL.8R.MER	3
5S.3B.6BL.8R.MER.WSC.WB	3
5S.3B.6BL.4.5R.LER	3
5S.3B.6BL.8R.LER	4
10S.3B.6BL.8R.HER	9
10S.3B.6BL.8R.HER.WSC.WB	9
10S.3B.6BL.4.5R.HER	9
10S.3B.6BL.4.5R.MER	9
10S.3B.6BL.8R.MER	9
10S.3B.6BL.8R.MER.WSC.WB	9
10S.3B.6BL.4.5R.LER	6